BMC Plant Biology

RESEARCH Open Access

# A single-cell transcriptome atlas reveals the transcriptionally earliest state in rice callus

Lan Lyu[1†], Wenrui Lou[1†], Wenkai Yan[2], Hengxiu Yu[3], Zhiyun Gong[4] and Yufeng Wu[1*]

## Abstract

**Background** The cell fate transition of pluripotent callus from somatic cells plays an important role in plant development studies and crop genetic improvement. Embryonic callus is a group of totipotent cells derived from the founder cells responsible for the initiation of callus. However, our understanding of the initial cellular states and regulatory factors of cell fate transition during callus development remains quite limited.

**Results** Single-cell RNA sequencing was employed to generate a single-cell transcriptome atlas of the rice (*Oryza sativa* L.) embryonic and differentiated callus. We found that the callus founder cell represented the transcriptionally earliest state of embryonic callus, which could transit into the root meristem niche, a process associated with starch degradation, lipid transport, energy production and transfer, plant hormones and flavonoid metabolism. The shoot meristematic cell represented the transcriptionally earliest state of differentiated callus, and these shoot meristematic cells differentiated into mesophyll precursor cells via vascular parenchyma cells, a process associated with chromatin-related epigenetic regulation, enzymatic reactions, signal transduction, metabolic activity and photosynthesis. The expression patterns of the genes involved in plant hormones, and *WUSCHEL RELATED HOMEOBOX* (*WOX*) family gene *DWARF TILLER1* (*OsDWT1*) across distinct cell populations suggested that gibberellin (GA) signaling and *OsDWT1* were associated with the callus founder cell fate transition.

**Conclusions** Our results revealed that the callus founder cell and shoot meristematic cell represent the transcriptionally earliest states of embryonic callus and differentiated callus in rice, respectively. This study provides preliminary resources for understanding the development of callus cells and offers clues for improving plant genetic transformation efficiency in recalcitrant rice varieties by regulating cell fate transition.

**Keywords** Single-cell, Transcriptome, Transcriptionally earliest state, Rice, Embryonic callus, Differentiated callus

[†]Lan Lyu and Wenrui Lou are contributed equally to this work.

*Correspondence:
Yufeng Wu
yfwu@njau.edu.cn
[1]State Key Laboratory for Crop Genetics and Germplasm Enhancement and Utilization, Bioinformatics Center, Academy for Advanced Interdisciplinary Studies, Nanjing Agricultural University, Nanjing 211800, China
[2]College of Horticulture, Henan Agricultural University, Zhengzhou 450002, China
[3]Jiangsu Key Laboratory of Crop Genomics and Molecular Breeding/Zhongshan Biological Breeding Laboratory/Jiangsu Co-Innovation Center for Modern Production Technology of Grain Crops, Agricultural College of Yangzhou University, Yangzhou 225009, China
[4]Jiangsu Key Laboratory of Crop Genomics and Molecular Breeding, Zhongshan Biological Breeding Laboratory, Key Laboratory of Plant Functional Genomics of the Ministry of Education, Agricultural College of Yangzhou University, Yangzhou 225009, China

## Introduction

Somatic embryogenesis is a morphogenetic process in which somatic cells are reprogrammed to develop into embryos capable of regenerating into whole plants. This phenomenon involves three key phases: the induction of embryonic callus, the maturation of somatic embryos, and their subsequent regeneration into complete plants. During this process, somatic cells regain totipotency through dedifferentiation and redifferentiation, with the formation of viable somatic embryos and their progression through developmental stages being critical for successful plant regeneration [1]. Under in vitro conditions, specific parenchyma cells within the callus differentiate into tubular cells, which may organize into vascular structures and ultimately contribute to organ formation. Consequently, the emergence of tubular cells during culture is recognized as an indicator of tissue differentiation [2].

The differentiation of plant cells is a critical stage in which totipotency enables cells to regenerate into complete plants. This process involves dynamic morphological changes and intricate molecular regulation. Recent advancements in single-cell RNA sequencing (scRNA-seq) have significantly advanced research in this field. In the dicot model plant *Arabidopsis thaliana*, studies on hypocotyl-derived callus revealed that the middle-layer cells exhibit transcriptome profiles highly similar to those of the root tip quiescent center (QC) [3]. *WUSCHEL RELATED HOMEOBOX 5/7* (*WOX5/7*) maintains stem cell properties in these cells and, through the *WOX5/7-PLETHORA* (*PLT*) protein complex, activates the auxin biosynthesis gene *TRYPTOPHAN AMINOTRANSFERASE OF ARABIDOPSIS1* (*TAA1*), promoting root differentiation [4]. Meanwhile, the shoot apical meristem (SAM) regulator *WUSCHEL* (*WUS*) is expressed in specific callus cells, facilitating shoot regeneration [5]. Additionally, ectopic activation of *WUS* and *DORNRÖSCHEN* (*DRN*) transcription factors enhances protoplast regeneration. These findings elucidate the molecular networks governing callus development in dicots [6].

In contrast, the in vitro induction process in monocots is more complex. Research on monocot models like rice has focused on genetic factors, culture medium composition, and callus browning mechanisms. For instance, japonica rice demonstrates superior callus induction and proliferation compared to indica rice [7], which makes it the most widely used variety in rice genetic transformation systems. Adjustments to sugar and nitrogen levels in culture media influence biomass accumulation in rice callus via the salicylic acid pathway [8], while increasing gene expression of *BROWNING OF CALLUS1* (*BOC1*) reduces oxidative stress-induced senescence to mitigate browning in rice callus induction [9]. Overexpression of maize morphogenic regulatory genes *Baby boom* (*Bbm*) and *Wuschel2* (*Wus2*) increases the transformation efficiency of maize and rice callus [10]. Recently, a plant elicitor peptide (REGENERATION FACTOR1, REF1) found in tomato has been shown to boost the regeneration and transformation efficiency of multiple difficult-to-transform crops including both dicots and monocots [11]. While these studies optimize genetic transformation systems across rice varieties, they have not addressed the cellular attributes of callus. Current transformation systems rely on the use of seed embryo explants that undergo dedifferentiation and redifferentiation, yet the cellular heterogeneity and transcriptional dynamics during these stages remain poorly characterized. Elucidating these features is essential for improving transformation efficiency and advancing functional genomics.

The rapidly advancing field of plant single-cell omics and trajectory inference methods has laid a technological foundation for exploring cell fate transition. Cuperus et al. employed Monocle and RNA Velocity to infer the developmental trajectory of root hair cells in *Arabidopsis* [12]. This study serves as an example how to accurately understand the expression patterns of individual cells and uncover cell fate transitions. A recent study based on a cross-organ single-cell multi-omics atlas of rice revealed that mesophyll cells in young leaves can differentiate into those in flag leaves, and that the initiation of differentiation is associated with transport- and environment-responsive factors by trajectory inference analysis [13].

To address the cellular heterogeneity and transcriptional features of rice seed embryo-derived callus at embryonic and differentiated stages, we used scRNA-seq to profile gene expression across these developmental states. We selected the *japonica* rice cultivar Nipponbare as the experimental system based on its dual advantages: a well-established efficiency in callus induction and differentiation, and the availability of extensive, high-quality multi-omics resources, which collectively provide an optimal foundation for robust single-cell transcriptomic profiling and subsequent in-depth analysis. The experimental design focused on dissecting cell fate transitions during in vitro culture to reveal the initial cellular states in rice callus. This approach provides critical insights into the molecular basis of totipotency expression in monocot cells.

## Methods

### Plant growth conditions

Mature seeds of *Oryza sativa* L. cv. Nipponbare were surface-sterilized sequentially with 70% ethanol (2 min) and 2% NaClO (20 min), followed by three rinses with sterile distilled water. Embryos were aseptically excised and cultured on induction medium for two weeks to induce callus formation. Embryonic callus was subsequently

sub-cultured on fresh induction medium (Murashige and Skoog medium [14] supplemented with 3% w/v sucrose, 0.25% w/v phytagel, 0.05% w/v casein hydrolysate, 2 μM 6-Benzylamino purine and 10 μM 2,4-dichlorophenoxyacetic acid, pH 5.8) at a growth chamber under 16-h dark, 28 °C/8-h dark, 24 °C cycle [15] for 7 days to establish embryonic callus with loose structure and a pale and translucent color. And the embryonic callus was transferred to differentiation medium (MS medium supplemented with 3% w/v sucrose, 3% w/v sorbitol, 0.25% w/v phytagel, 0.05% w/v casein hydrolysate, 10 μM 6-Benzylaminopurine and 1 μM zeatin, 2 μM kinetin, 1 μM 1-Naphthaleneacetic acid, 4 μM glutamine, 4 μM proline, pH 5.8) containing at a growth chamber under 16-h light, 28 °C/8-h dark, 24 °C cycle for 7 days to establish differentiated callus with compact structure and distinct green spots. The embryonic callus and differentiated callus were prior to downstream analyses. For bulk RNA-seq, three biological replicates from each callus were performed.

#### Histological morphology analysis

Small callus fragments were embedded in Optimal Cutting Temperature compound (OCT), and their orientation was adjusted before placement in the freezing chamber of a Leica CM1950 cryostat. The chamber temperature was set to −24 °C, and the sample head temperature to −20 °C. After complete freezing, the embedded blocks were mounted onto the sample head. The stage tilt angle and section thickness were adjusted for trimming. When nearing the sample, the section thickness was set to 10 μm for formal sectioning. Sections were then transferred to slides, ensuring sample integrity and flatness throughout the rapid process.

Slides were dried at 37 °C, followed by incubation in pre-chilled methanol for 30 min. After removal, 500 μL of isopropanol was added, and slides were incubated at room temperature for 1 min. The solution was discarded, and 1 mL of 0.05% (w/v) toluidine blue staining solution was applied to fully cover the tissue [16]. After 1-min staining at room temperature, excess dye was removed, and slides were rinsed in sterile water to eliminate residual stain. Finally, slides were dried at 37 °C and imaged under bright-field microscopy using an Olympus MVX10 fluorescence microscope.

#### Protoplast isolation and single-Cell RNA sequencing

Callus tissues were dissected into small fragments and enzymatically digested in a solution containing 1.5% (m/v) cellulase R10, 0.75% (m/v) macerozyme R10, 0.8 M mannitol, 10 mM MES (pH5.7), 10 mM $CaCl_2$, 0.1% (m/v) BSA, and 0.04% 2-mercaptoethanol at 37 °C for 30 min. The digested suspension was filtered through a 70 μm cell strainer twice, followed by centrifugation at 130 × g for 5 min to pellet cells. The supernatant was discarded, and the pellet was resuspended in 8% mannitol solution. This washing step was repeated three times. The final cell pellet was resuspended in 8% mannitol to achieve optimal concentration. Cell viability and concentration were assessed by staining 1–2 μL of the suspension with trypan blue and analyzing under an Olympus MVX10 fluorescence microscope.

A 20 μL aliquot of protoplast suspension (700 cells/μL, viability > 90%) was loaded into a 10X Genomics microfluidic chip. Protoplasts, gel beads with barcodes, and reaction reagents were encapsulated into oil droplets. Following lysis within droplets, RNA was reverse-transcribed into cDNA and tagged with barcodes. Oil droplets were disrupted, and cDNA was PCR-amplified. Amplified products underwent quality control (QC), and qualified samples were fragmented into 200–300 bp segments. Fragments were end-repaired, A-tailed, and ligated with P7 adapters. Index sequences were added via PCR, followed by fragment size selection and final QC. The library was sequenced on an Illumina HiSeq platform using paired-end (PE100) mode. Raw sequencing data comprised Read1 (26 bp: 16 bp barcode + 10 bp UMI), Read2, and the i7 index.

#### Processing of scRNA-seq data

The raw scRNA-seq dataset was first analyzed by Cell Ranger 7.1.0 (10X Genomics) with the rice genome (https://ftp.ensemblgenomes.ebi.ac.uk/pub/plants/release-56/gff3/oryza_sativa/). These pipelines include processing of raw scRNA-seq data to align reads and generate gene-cell matrices. Run 'cellranger mkref' with "–genome, –fasta and –genes" arguments to build reference. Run 'cellranger count' with "–id, –transcriptome, –fastqs, –sample and –force-cells = 10,000" arguments to generate single-cell gene counts. 97.5% reads of embryonic callus and 97.7% reads of differentiated callus were aligned to the rice reference genome. Mean reads per cell were 84,228 and 84,142. Median genes per cell were 3,457 and 4,385. The gene-cell matrices 'filtered_gene_bc_matrices' which was named by 10X Genomics generated by Cell Ranger 7.1.0 served as raw data for downstream analyses.

#### Cell clustering

The gene-cell matrices of 10,000 cells were load into the Seurat 4.3.0.1, which was implemented in R 4.2.3. To remove dead cells and doublets, we filtered genes expressed in less than three cells, and cells with more than 10,000 genes expressed, less than 500 genes expressed, have more than 50,000 UMI counts and have less than 500 UMI counts, less than 15% mitochondrial genes expressed and less than 3% chloroplast genes expressed were kept. After filtering, 9,888 cells and 9,936 cells were used for downstream analysis. The scaled data were first

normalized by LogNormalize. The highly variable genes were calculated by "FindVariableFeatures" with default parameters. A total of 2,000 highly variable genes were used for clustering analysis. Clusters were identified by "FindClusters" with "FindNeighbors_dim = 15, resolution = 0.5, tsne_dim = 10, umap_dim = 10". The differential expression genes of cell types were identified with "logfc_threshold = 0.25, min_pct = 0.1, test_use = "wilcox", only.pos = TRUE. Criteria were used: filter.p_val_adj = 0.05, filter.avg_log2FC = 0.25, filter.pct1 = 0.1, filter.pct2 = 0.5.

#### Trajectory analysis

We used PAGA of the Python package Scanpy to generate nodes representing cell clusters and edge weights representing the confidence in the existence of connections between cell clusters for trajectory inference [17]. First, the single-cell expression matrix was normalized and dimensionality reduction was performed to construct a neighborhood graph among cells. Then abstract the cell-level graph into a cluster-level graph and compute the connectivity strength between clusters to infer cell developmental trajectories and branch points based on the abstracted graph with default parameters. RNA velocity enables the recovery of directed dynamic information by leveraging splicing kinetics [18]. With velocyto, the BAM format output files from Cell Ranger were converted into the loom format, which is then input into scVelo for calculating RNA velocity under default parameters. The number of detected RNA splicing events per cell was quantified to predict the gene-splicing rate in each cell to construct velocity graph and perform visualization in two-dimensional UMAP space. The Monocle 2 package was used to deeply analyze the process of cell fate transition [19]. The subset of raw data was extracted with cluster information to explore cell fate transition of related clusters. First, the variance in each gene's expression across cells was calculated by running "dispersionTable". Based on average expression level, variable genes were chosen to define a developmental progress with default parameters. Then, the data's dimensionality was reduced to two components. The transition of cells from one state to another was described in a lower dimensional space, and the cells were ordered in pseudo-time by calling "orderCells". For specifying a priori "beginning" of the trajectory of the tree, run 'orderCells' again setting the "root_state" argument. The genes that were significantly enriched were visualized by heatmap. The data used for plotting heatmap were also used for GO biological process analyses using GO annotation database from TBtools V1.120. All annotated genes were used as background.

#### Hormone genes expression analysis

The gene expression pattern of hormone genes in rice across callus cell types were scored by UCell [20] which depends only on the relative gene expression in individual cells and are therefore not affected by dataset composition.

## Results

#### Assembly of single cell transcriptome atlas in rice callus

The embryonic and differentiated callus were distinguished by histological analysis. Callus displayed a loose, light-colored, and translucent morphology (Fig. 1A), suggesting the callus corresponds to the embryonic state. This observation confirmed through frozen sections stained with toluidine blue for cellular characterization. The embryonic callus comprised uniformly shaped cells with even, darker staining (Fig. 1B). The differentiated callus exhibited a compact, darker structure with distinct green spots (Fig. 1C), and displayed irregular cell morphologies, uneven staining, and lighter coloration. Notably, tightly arranged tubular cells with smaller sizes and intense staining were observed in differentiated callus (Fig. 1D).

Embryonic and differentiated callus samples from multiple biological individuals were pooled, respectively, to represent the average state prior to protoplast isolation for scRNA-seq. An initial quality assessment of the single-cell transcriptome data was performed using the 10X Genomics Cell Ranger pipeline, targeting an initial set of 10,000 cells. Barcode rank plots were used to distinguish real cells from background or empty droplets. The number of genes detected in both tissues dropped sharply beyond approximately 10,000 cells (Table 1, Supplemental Fig. S1A, B), indicating a significant difference between intact cells and the background. Data quality metrics, such as the mean reads per cell, the median number of genes per cell, and the median UMI count per cell, were similar to those of rice root tip cells [21]. To further assess data quality, we performed bulk RNA-seq on both embryonic and differentiated callus samples and treated the scRNA-seq as pseudo bulk RNA-seq. The correlation coefficients between the two datasets were all greater than 0.6, indicating that our scRNA-seq data overall recapitulated the expression profiles of the two samples with high reliability (Supplemental Fig. S1C, D). After filtering (see methods), 9,888 cells from embryonic callus and 9,936 cells from differentiated callus were used for subsequent cell clustering, yielding six clusters for embryonic callus and six clusters for differentiated callus.

#### Cell-type annotation

Two types of callus cells were clustered into distinct populations based on their single-cell transcriptome profiles to explore the cellular properties of rice callus tissues.

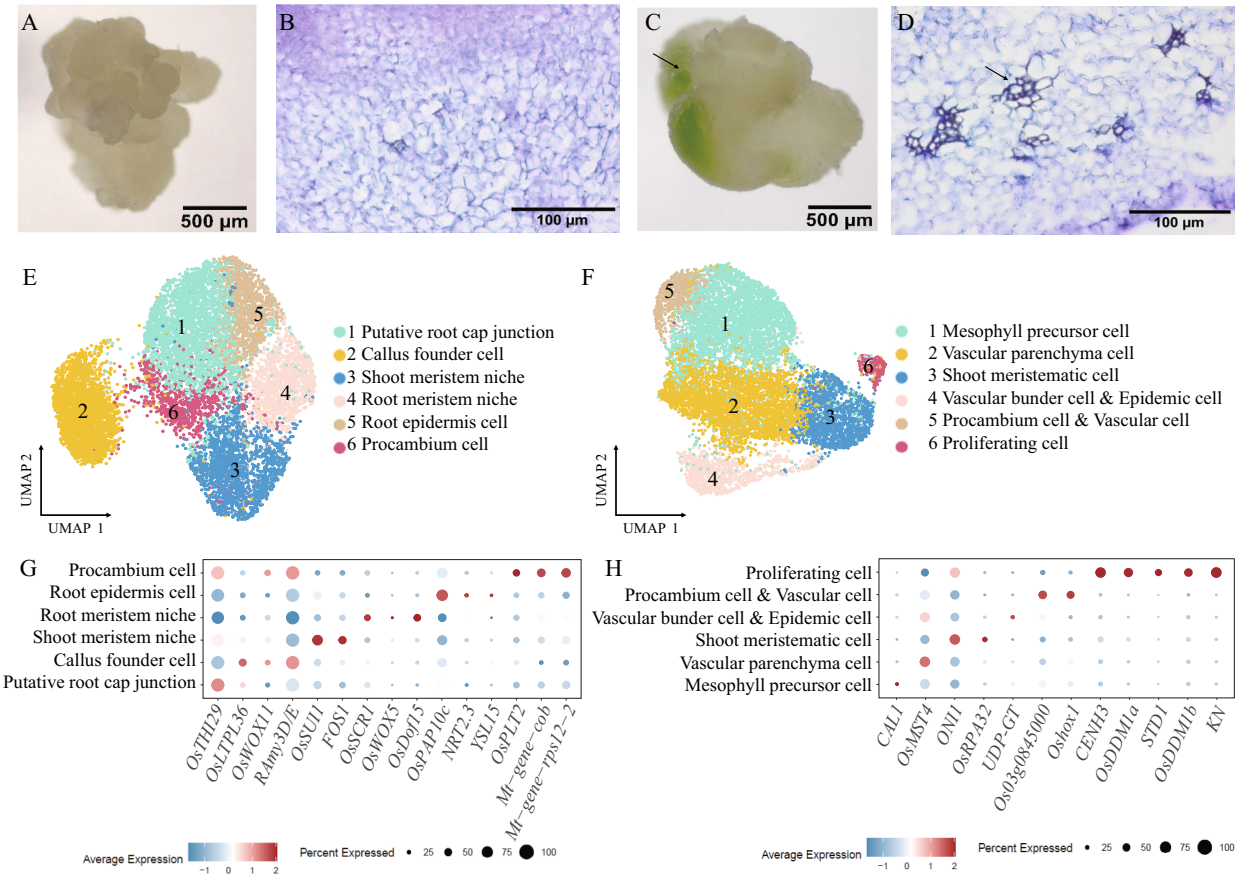


**Fig. 1** Profiling single-cell transcriptome atlas in rice callus. Overview of experimental samples (**A**-**D**). Tissue morphology of rice embryonic callus. The embryonic callus stained by toluidine blue (**A**, **B**). Tissue morphology of rice differentiated callus (**C**, **D**). The arrow points to green shots. And the differentiated callus stained by toluidine blue, the arrow points to tuber cells. **A**, **C** Bar = 500 μm; **B**, **D** Bar = 100 μm. Two-dimensional embedding of transcriptome similarity among cell with uniform manifold approximation and projection (UMAP) (**E**, **F**), cells are colored by cluster identity. UMAP embedding of cell colored by cluster identity of rice embryonic callus (**E**). UMAP embedding of cell colored by cluster identity of rice differentiated callus (**F**). The expression pattern of marker genes in each cluster by dot-plot (**G**, **H**), the point indicates marker genes of cell clusters in rice callus and the shades of color denote the expression level of marker genes in cell clusters. The expression pattern of marker genes in rice embryonic callus (**G**). The expression pattern of marker genes in rice differentiated callus (**H**)

**Table 1** The statistics on the data of scRNA-seq in rice callus

| Tissue | Number of cells | Mean reads/cell | Median genes/cell | Total genes | Median UMI/cell |
|---|---|---|---|---|---|
| C | 9,888 | 84,228 | 3,457 | 29,591 | 11,724 |
| Cg | 9,936 | 84,142 | 4,385 | 31,077 | 15,284 |

C-embryonic callus, Cg-differentiated callus

Due to the absence of known marker genes for rice callus cell types, the cell populations in both callus types were annotated by compiling and analyzing published cell type-specific marker genes and in situ hybridization data from other rice tissues (Fig. 1E, F).

In embryonic callus, the putative root cap junction marker gene *THIONIN29* (*OsTHI29*) [22] was specifically expressed in cell cluster 1 (Fig. 1G, Supplemental Fig. S2A), therefore, cell cluster 1 was annotated as putative root cap junction cells. The specific expression of several genes in cluster 2 led to its annotation as callus founder cells. These included: *OsLTPL36*, whose homolog in *Arabidopsis* is specifically expressed in early-stage callus initiation cell [2]; *OsWOX11*, a homolog of callus founder cell marker gene *WOX11* in *Arabidopsis* [23]; and the α-amylase gene *ALPHA-AMYLASE3D/E* (*RAmy3D/E*), which expresses in scutella epithelium cells of callus-forming rice embryos by in situ hybridization [24]. In cell cluster 3, the meristem niche-expressed gene *OsSUI1*, a rice translation initiation factor SUI gene [25] and the gene *FON2 SPARE1* (*FOS1*) [26], which maintains shoot apical meristem activity, were specifically expressed, resulting in its classification as the shoot meristem niche. Root meristem activity maintenance-related genes *SCARECROW1* (*OsSCR1*), *OsWOX5*, and *DNA BINDING WITH ONE FINGER15* (*OsDof15*) were specifically expressed in cell cluster 4 [27–30], leading to its annotation as the root meristem niche. The gene *PURPLE ACID PHOSPHATASE10C* (*OsPAP10c*), encoding a purple acid

**Table 2** The marker genes of cell clusters in rice embryonic callus

| Cell Cluster | Annotation of Cell Type | Marker Genes & Reference |
|---|---|---|
| Cluster1 | Putative root cap junction | *OsTHI29* [22] |
| Cluster2 | Callus founder cell/Primordial cell | *OsLTPL36*, *OsWOX11*, *RAmy3D/E** [2, 23, 24] |
| Cluster3 | Shoot meristem niche | *UNP1*, *FOS1* [25, 26] |
| Cluster4 | Root meristem niche | *OsSCR1*, *OsWOX5*, *OsDof15* [27–30] |
| Cluster5 | Root epidermis cell | *OsPAP10c*, *NRT2.3*, *YSL15* [31–33] |
| Cluster6 | Procambium cell/Formative cell | *OsPLT2*, *Mt-gene-cob*, *Mt-gene-rps12-2* [27, 34] |

An asterisk (*) indicates evidence based on in situ hybridization; all other markers are supported by literature evidence

**Table 3** The marker genes of cell clusters in rice differentiated callus

| Cell Cluster | Annotation of Cell Type | Marker Genes & Reference |
|---|---|---|
| Cluster1 | Mesophyll precursor cell | *CAL1* [35] |
| Cluster2 | Vascular parenchyma cell | *OsMST4** [36] |
| Cluster3 | Shoot meristematic cell | *ONI1*, *OsRPA32* [37, 38] |
| Cluster4 | Vascular bunder cell & Epidemic cell | *UDP-GT* [36] |
| Cluster5 | Procambium cell & Vascular cell | *Os03g0845000*, *Oshox1* [35, 39] |
| Cluster6 | Proliferating cell | *CENH3*, *OsDDM1a/b*, *STD1*, *KN* [36, 40, 41] |

An asterisk (*) indicates evidence based on in situ hybridization; all other markers are supported by literature evidence

phosphatase associated with root surface secretion [31], was specifically expressed in cell cluster 5. Furthermore, epidermal marker genes *HIGH-AFFINITY NITRATE TRANSPORTER2.3* (*NRT2.3*) and *YELLOW STRIPE LIKE15* (*YSL15*) were also specifically expressed in cell cluster 5 [32, 33] (Fig. 1G). *OsNRT2.3* encodes a component of the high-affinity nitrate transport system (HATS) in rice, influencing nitrogen uptake in root cells [33], while *OsYSL15* is strongly induced by iron deficiency and is active in all tissues except epidermal cells under low iron conditions [32]. Therefore, cell cluster 5 was defined as root epidermis cells. Finally, the stem cell marker gene *PLETHORA 2* (*OsPLT2*), promoting cell proliferation during root primordia development was specifically expressed in cell cluster 6 [27, 34], leading to the annotation of cell cluster 6 as procambium cells (Table 2).

In differentiated callus, the mesophyll precursor cell marker gene *CADMIUM ACCUMULATION IN LEAF1* (*CAL1*) was specifically expressed in cell cluster 1 [35] (Fig. 1H, Supplemental Fig. S2 B). Therefore, cell cluster 1 was defined as mesophyll precursor cells. In situ hybridization experiments showed that the gene *MONOSACCHARIDE TRANSPORTER4* (*OsMST4*) accumulates in vascular parenchyma cells. This gene was specifically expressed in cell clusters 2 [36], leading to the annotation of cell cluster 2 as vascular parenchyma cells. In cell cluster 3, shoot apical meristem marker gene *ONION1* (*ONI1*) [37] and the meristem cell marker gene *REPLICATION PROTEIN A32* (*OsRPA32*) were specifically expressed [38], leading to its classification as shoot meristematic cells. The vascular bundle and epidermic cell marker gene *UDP-GLUCOSYLTRANSFERASE* (*UDP-GT*) [36] was specifically expressed in cell cluster 4. Therefore, cell cluster 4 was annotated as vascular bunder cells and epidemic cells. In cell cluster 5, the vascular cell marker gene *Os03g0845000*, and the procambium marker gene *HOMEOBOX1* (*Oshox1*) were specifically expressed [35, 39]. Thus, cell cluster 5 as procambium cells and vascular cells. In cell cluster 6, proliferating cell marker genes *STEMLESS DWARF1* (*STD1*) and *KNOLLE* (*KN*) were specifically expressed [36, 40, 41]. Rice *STD1* is homologous to *Arabidopsis PAKRP2* and is primarily expressed in actively dividing tissues. *std1* mutants exhibit severe dwarfism, abnormal cell shapes, and reduced cell division rates [41]. Therefore, cell cluster 6 was defined as proliferating cells (Table 3).

Thus, we have constructed a single-cell transcriptome atlas that reveals cell heterogeneity, which will help to facilitate the findings of rice callus initial cellular states, cell fate transition and exploration of the regulators of functional cell types.

### The developmental trajectory of the callus founder cell population

Previous studies have shown that in rice tissue culture, scutellum-derived callus originates from scutella epidermal cells [42, 43], with evidence suggesting the co-option of embryonic developmental pathways during initiation [44, 45]. To investigate embryonic callus formation, we reconstructed developmental trajectories based on RNA velocity (see methods), revealing that embryonic callus potentially develops from callus founder cells to procambium cells (Fig. 2A). Pseudo-temporal ordering of the two cell types demonstrated that callus founder cells occupied the early pseudo-time (Fig. 2B), implying its transcriptionally earliest state for embryonic callus.

Meanwhile, gene expression dynamics along the trajectory showed that the family member genes of the callus founder cell marker gene (*RAmy3D/E*) enriched in early pseudo-time, while the family member genes of the specific expressed marker genes of procambium cell (*Mt-gene-rps12-2*) (Fig. 1G) peaked in later pseudo-time (Fig. 2C). We also found that embryogenesis-related genes *LATE EMBRYOGENESIS ABUNDANT PROTEIN GENES* (*OsLEAs*) [46] and lipid transfer protein genes *LIPID TRANSFER PROTEIN GENES* (*OsLTPs*) [45] were enriched in early pseudo-time (Fig. 2C, Supplemental

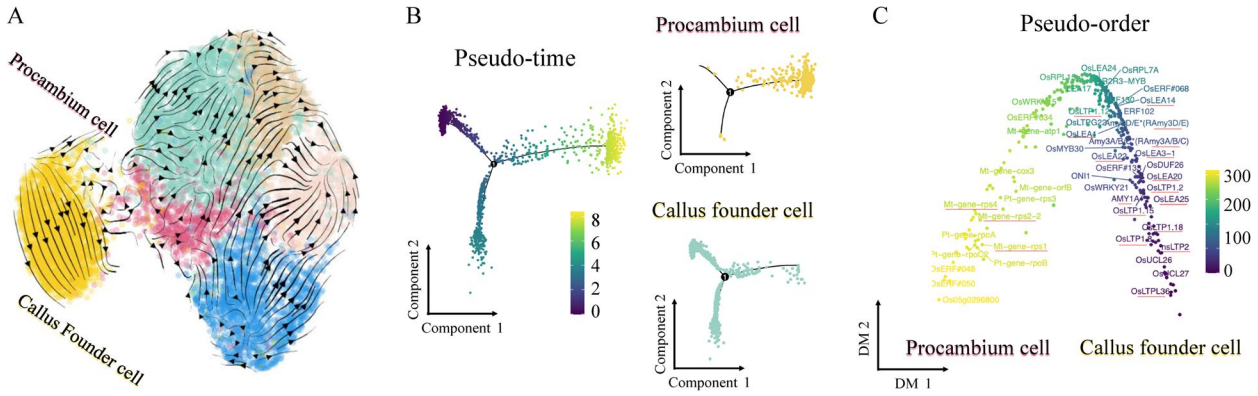


**Fig. 2** Developmental trajectory analysis of callus founder cell. The cell trajectory analysis of embryonic callus by RNA velocity analysis. Arrowheads indicate predicted differentiation trajectories. Arrowheads indicate predicted differentiation trajectories (**A**). The cell trajectory analysis of callus founder cell and procambium cell. The color intensity indicates the developmental timing, where darker colors represent earlier stages of development (**B**). The hypervariable expression gene along cell trajectory (**C**), the light and dark of the color dedicates the time of cell fate transition. The red underlined genes are the family member genes of the specific expressed marker gene of procambium cell (*Mt-gene-rps*12-2) and the family member genes of callus founder cell marker gene (*RAamy3D/E*), embryogenesis-related genes *OsLEAs* and lipid transfer protein genes *OsLTPs*

Table S1), which is corroborated by known high *OsLTP1* expression in scutellum-derived callus [44], suggesting the potential function of the callus founder cell was associated with starch catabolism, lipid transport, and embryogenesis.

To elucidate the cell fate transition between callus founder cells and procambium cells, subpopulation analysis was performed on both cell groups. The results revealed that procambium cells consisted of Subclusters 1 and 4, while callus founder cells comprised Subclusters 2, 3, and 5 (Fig. 3A). Cell lineage analysis of these subpopulations exhibited two potentially distinct fate transition paths: one toward Subclusters 1 and 4, and the other toward Subclusters 3 and 2. Additionally, Subclusters 1 and 3 showed bidirectional connectivity in their differentiation paths, potentially. Pseudo-temporal analysis showed that Subcluster 5 was in the early pseudo-time (Fig. 3B, C), suggesting that Subcluster 5 was in transcriptionally earliest state. These results indicated that callus founder cells were originated from Subcluster 5.

Prior studies contextualize the findings that *APETALA2/ETHYLENE RESPONSIVE FACTOR* (*ERF*) transcription factors are essential for *Arabidopsis* callus formation, *WOX5/7* mutations impair regeneration, and *OsLTPs* show high expression in rice scutellum-derived callus [47]. Analysis of these genes' expression pattern across subclusters (Fig. 3D) and along Subcluster5-derived trajectories (Fig. 3E) identified that *OsWOX11* specifically was expressed in Subcluster5, *RAmy3A/B/C* was enriched in Subcluster4, and *OsLTP1.15* and *OsDWT1* were elevated in Subcluster2. *OsWOX11* peaks at early pseudo-time, suggesting it maintains embryonic competence. *RAmy3A/B/C* shows sustained high expression with maxima at early and upper branches of Branch Points1/2, indicating energy provision for the callus founder cell. *OsDWT1* exhibits baseline-low expression but sharp peaks near Branch Point1. *OsLTP1.15* maintains uniform expression across pseudo-time, matching the expression in transitional Subclusters 1/3, implicating a role in lipid transport during cell fate transition.

### Establishment of cellular identity of the root meristem niche in rice embryonic callus

Building on evidence that Arabidopsis leaf-derived callus resembles the root apical meristem [48] and that lateral root primordium-initiating (LRPI)-like cells and quiescent center (QC)-like cells are responsible for initiating early callus formation. LRPI-like cells are derived from xylem pole pericycle cells and are similar to lateral root primordia, genes encoding the lipid transporters LTP1 and LTP2 were highly enriched in LRPI-like cells [3]. Based on our prior annotation confirming the presence of root meristem niche cells in rice embryonic callus, we subsequently explored their cell fate determination by ordering callus founder cells, procambium cells, and root meristem niche cells along pseudo-time. Trajectory analysis revealed a bifurcation at the branch point with callus founder cells and the sparse population of procambium cells localized to early pseudo-time, while root meristem niche cells and a minimal number of procambium cells were located along one branch, and procambium cells with sparse callus founder cells occupied the other branch (Fig. 4A). Density visualization confirmed a sequential stratification: callus founder cells dominated the early pseudo-time, procambium cells the mid-pseudo-time and root meristem niche cells the late pseudo-time (Fig. 4B), indicating that root meristem niche cells are formed from callus founder cells via procambium cells.

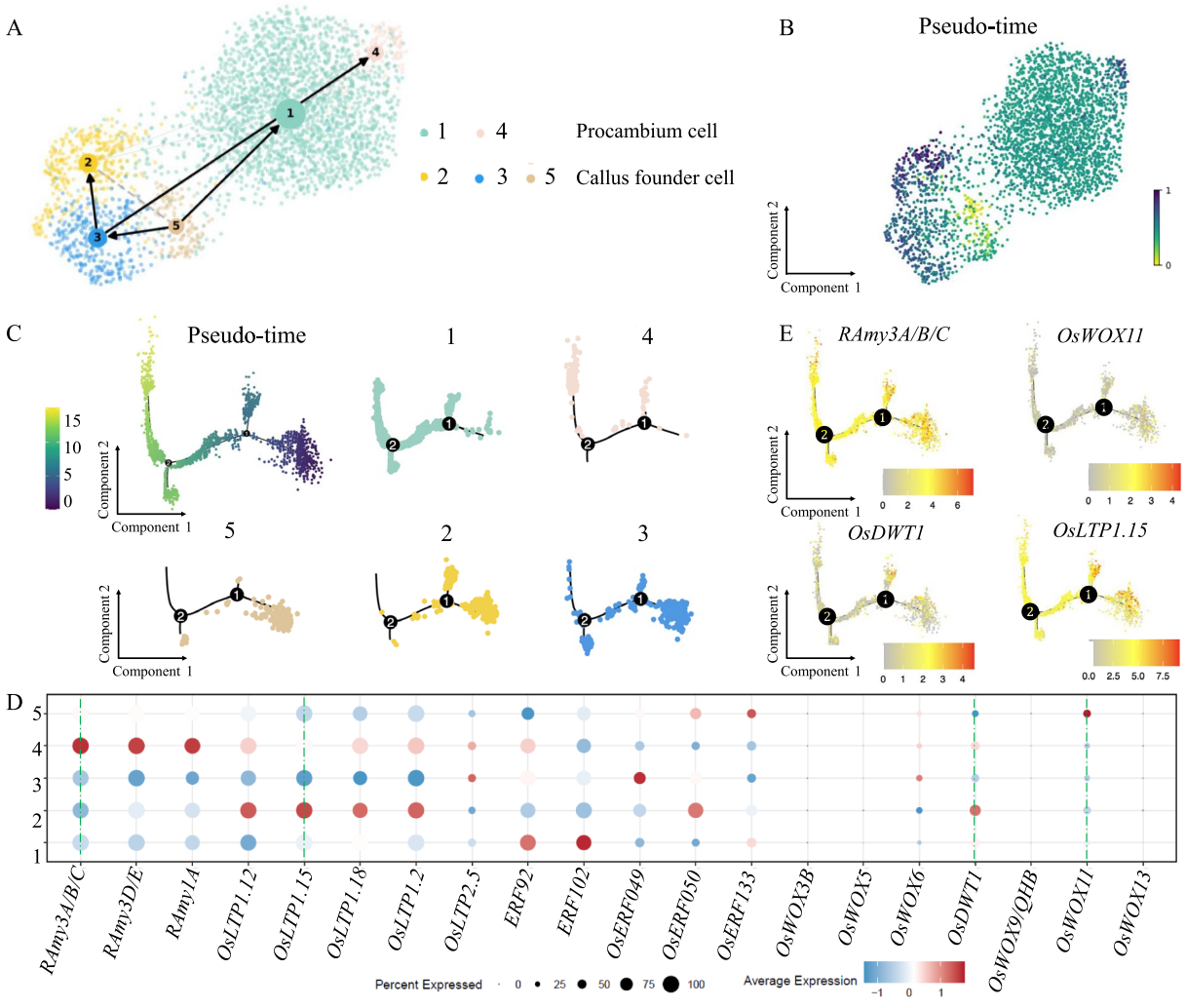


**Fig. 3** Subcluster analysis of callus founder cell. The cell lineage of the cell subclusters in callus founder cell and procambium cell predicted by PAGA (**A**), the nodes represent cell clusters, and edge weights represent confidence in the existence of connections between cell clusters. Visualizing the fate transition of subclusters in two-dimensional space. **B**. The brighter the color, the shorter the differentiation time. The cell trajectory analysis of the cell subclusters in callus founder cell and procambium cell by Monocle2. Distribution of the cell subclusters on the pseudo-time trajectory branches (**C**). The gene expression pattern in the cell subclusters of callus founder cell and procambium cell. Dots represent genes, with redder colors indicating higher gene expression levels (**D**). The dashed green line implies *RAmy3A/B/C*, *OsWOX11*, *OsDWT1* and *OsLTP1.15* (**G**). *RAmy3A/B/C*, *OsWOX11*, *OsDWT1* and *OsLTP1.15* expression pattern along the pseudo-time of the cell subclusters. Redder colors indicating higher gene expression levels

Next, we analyzed gene expression patterns along the reconstructed developmental trajectories, identifying six gene expression clusters (Fig. 4C). During the early pseudo-time along the trajectory from callus founder cells to root meristem niche cells, the Gene Ontology (GO) terms enriched for the genes from cluster 1, 2, 3 were related to the carbohydrate metabolism, lipid transport, auxin and GA responsiveness. The representative genes included *SMALL AUXIN-UP RNA2* (*OsSAUR2*), *GA-ENHANCED GENE1* (*OsGAE1*) [49, 50], *OsLTP1.18/1.15* [44, 51], *RAmy3D/E* [25, 45]. The enriched GO terms for genes in cluster 1, 2 were consistently related to the functions of marker genes of callus founder cells. These results indicated that the plant hormones, auxin and GA potentially involved in the cell fate transition of the callus founder cell population.

### The development of shoot meristematic cells in differentiated callus

To explore the cell developmental trajectories in differentiated callus, we performed trajectory analysis which revealed that shoot meristematic cells were at the putative root of the trajectory with trilineage: one branch led toward proliferating cells, another toward mesophyll precursor and vascular cells, and the third toward bundle sheath and epidermic cells (Fig. 5A). The results suggested that shoot meristematic cells were the putative root of the trajectory in differentiated callus. Given

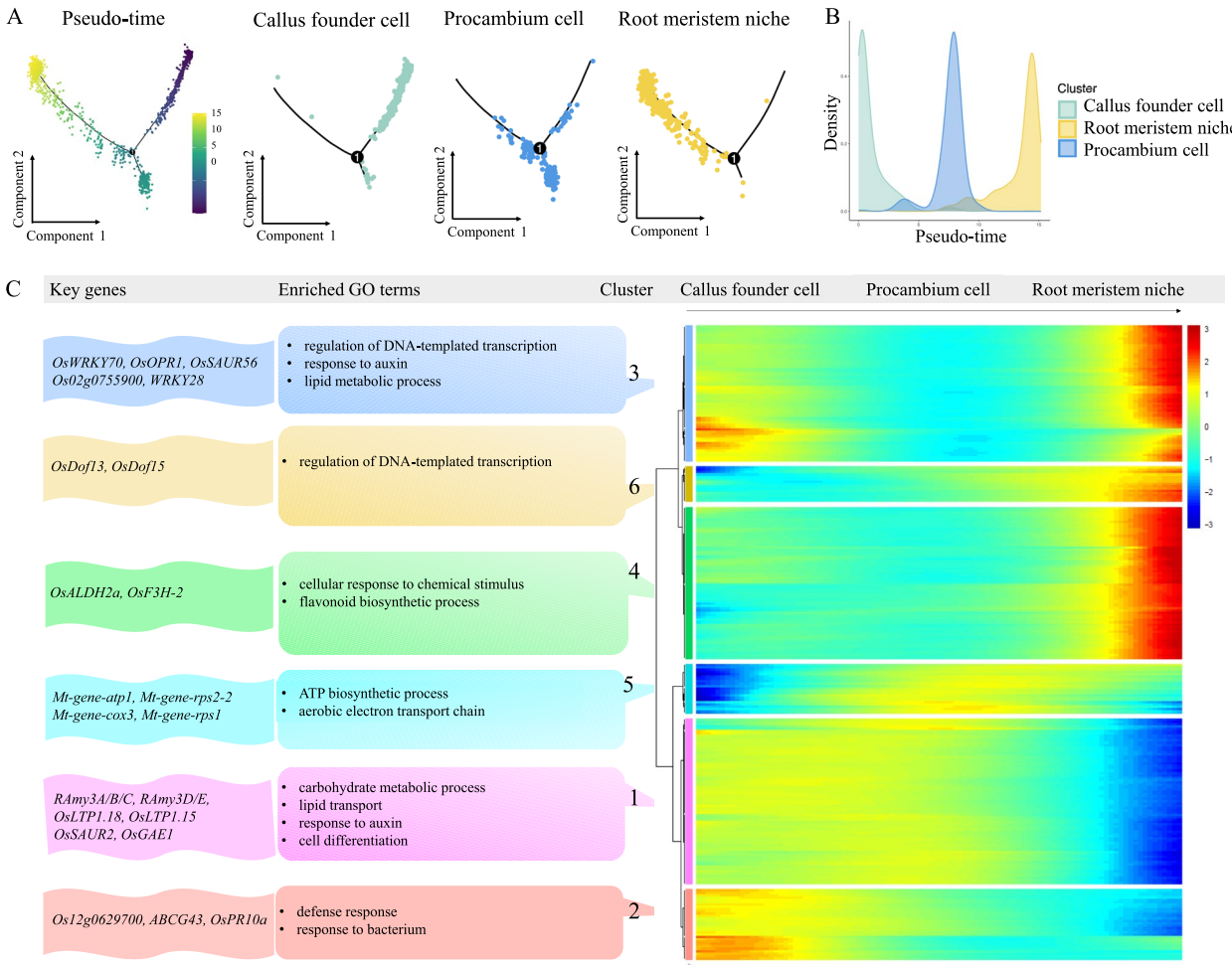


**Fig. 4** Establishment of cellular identity of root meristem niche in rice embryonic callus. The cell trajectory analysis of callus founder cell, procambium cell and root meristem niche (**A**). The color intensity indicates the developmental timing, where darker colors represent earlier stages of development. Distribution of the callus founder cell, procambium cell and root meristem niche along the pseudo-time trajectory. Heatmap displaying changes in gene expression along the pseudo-time trajectory branches (**B**). These genes were clustered into six modules with distinct expression patterns. The light and dark of the color represents the level of gene expression

the multipotency of mesophyll precursor cells in developing photosynthetic tissues [52], we ordered shoot meristematic cells, vascular parenchyma cells, mesophyll precursor cells, procambium cells & vascular cells along pseudo-temporal trajectory (Fig. 5B). The result exhibited a bifurcation at branch point 3, and shoot meristematic cells, vascular parenchyma cells, and a sparse population of mesophyll precursor cells distributed at early pseudo-time. Density visualization confirmed that shoot meristematic cells dominated early pseudo-time, vascular parenchyma cells the mid-pseudo-time, and mesophyll precursor cells & procambium cell the late pseudo-time, with a sparse population of procambium cells persisting in the early phases (Fig. 5C).

Gene expression patterns along the reconstructed developmental trajectories revealed that the genes of cluster 1 and 2, such as *DWARF AND LOW-TILLERING* (*DLT*), *LONELY GUY1*(*LOG1*), *DWT1*, *KN*, *STD1*, *CENTROMERIC HISTONE3* (*CENH3*), *DECREASE IN DNA METHYLATION1A* (*OsDDM1a*) [25, 42–46] (Fig. 5D), were enriched in the early pseudo-time. The GO terms of these genes were related to the regulation of chromatin binding and cell cycle. In the late pseudo-time of the trajectory where shoot meristematic cells transiting to mesophyll precursor cells, genes in cluster 5 and 6 were associated with many GO terms related to precursor metabolism and photosynthesis including *Pt-gene-rpl20*, *HYBRID PROLINE-ORGLYCINE-RICH PROTEIN21* (*OsHyPRP21*), *RICE SQUAMOSA PROMOTER-BINDING-LIKE7* (*SPL7*) [36, 53, 54]. These results implicated chromatin-mediated epigenetics is associated with the early stage of shoot meristematic cell fate transition, and that the photosynthesis and metabolism pathways are the potential regulatory factors in mesophyll precursor cells specification.

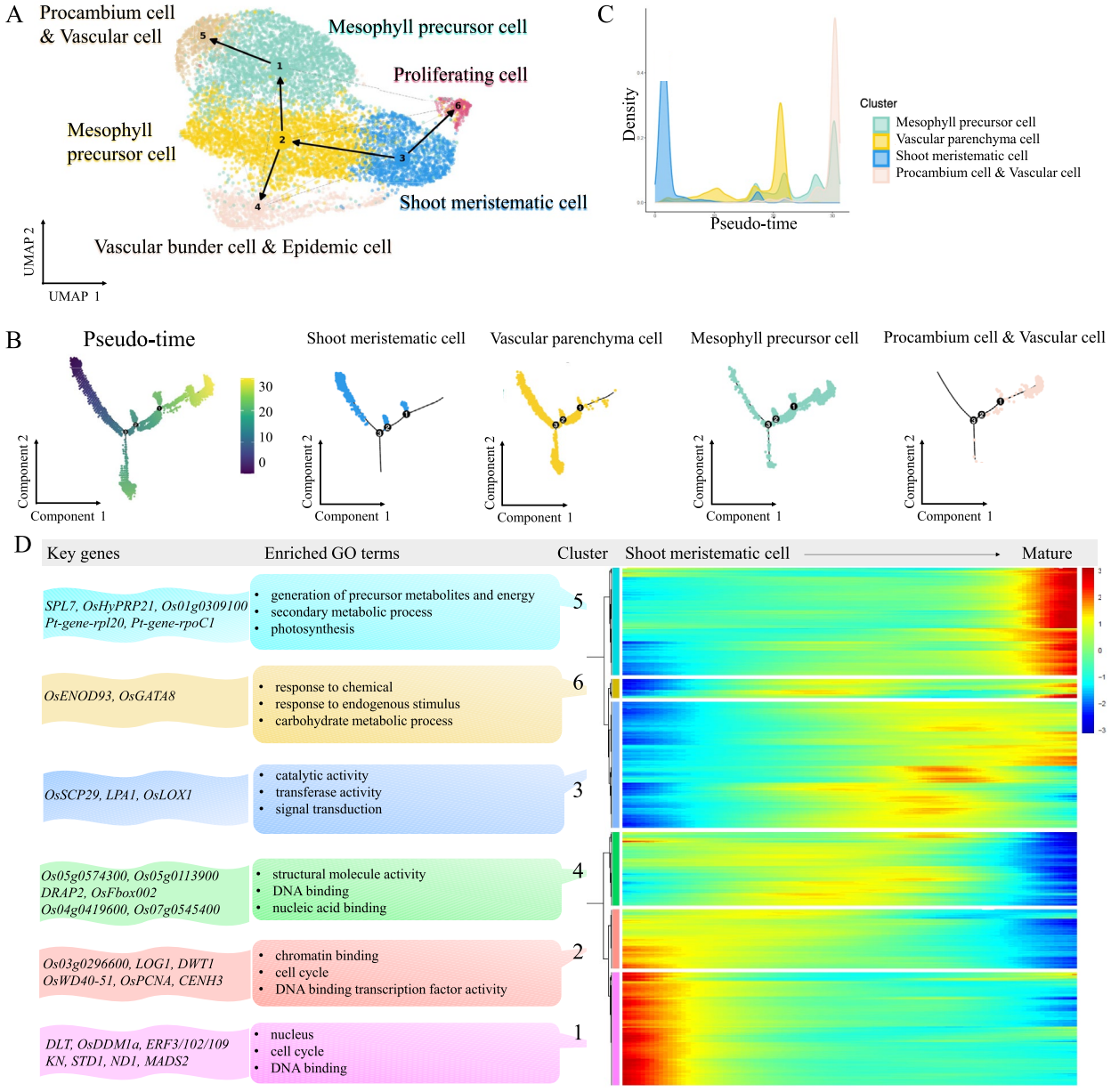


**Fig. 5** Developmental trajectory analysis of cells in rice differentiated callus. The cell lineage of rice differentiated callus cell predicted by PAGA, the nodes represent cell clusters, and edge weights represent confidence in the existence of connections between cell clusters (**A**). The cell trajectory analysis of shoot meristematic cell, vascular parenchyma cell, mesophyll precursor cell, procambium cell & vascular cell. The darker colors represent earlier stages of development (**B**). Distribution of shoot meristematic cell, vascular parenchyma cell, mesophyll precursor cell, procambium cell & vascular cell along the pseudo-time trajectory (**C**). Heatmap displaying changes in gene expression along the pseudo-time trajectory branches (**D**). The genes were clustered into six modules with distinct expression patterns. The light and dark of the color represents the level of gene expression

### *OsDWT1* was associated with callus founder cell fate transition

Plant hormones—including auxin, ethylene, GA, abscisic acid (ABA), and brassinosteroids (BR)—orchestrate callus differentiation [55, 56]. To identify key regulators of rice callus cell differentiation, we analyzed the expression patterns of phytohormone biosynthesis and responsive genes of rice (Supplemental Table S2) across both callus cell types by UCell [20]. In embryonic callus, BR and GA responsive genes showed specific expression in callus founder cells (Fig. 6A). In differentiated callus, auxin synthesis and ethylene responsive genes displayed specific expression in shoot meristematic cells (Fig. 6B), implying cell-type-specific phytohormone dynamics.

The broad developmental functions of WOX transcription factors, which are implicated in embryogenesis, vegetative growth, reproductive development, and seed production, are closely linked to phytohormone

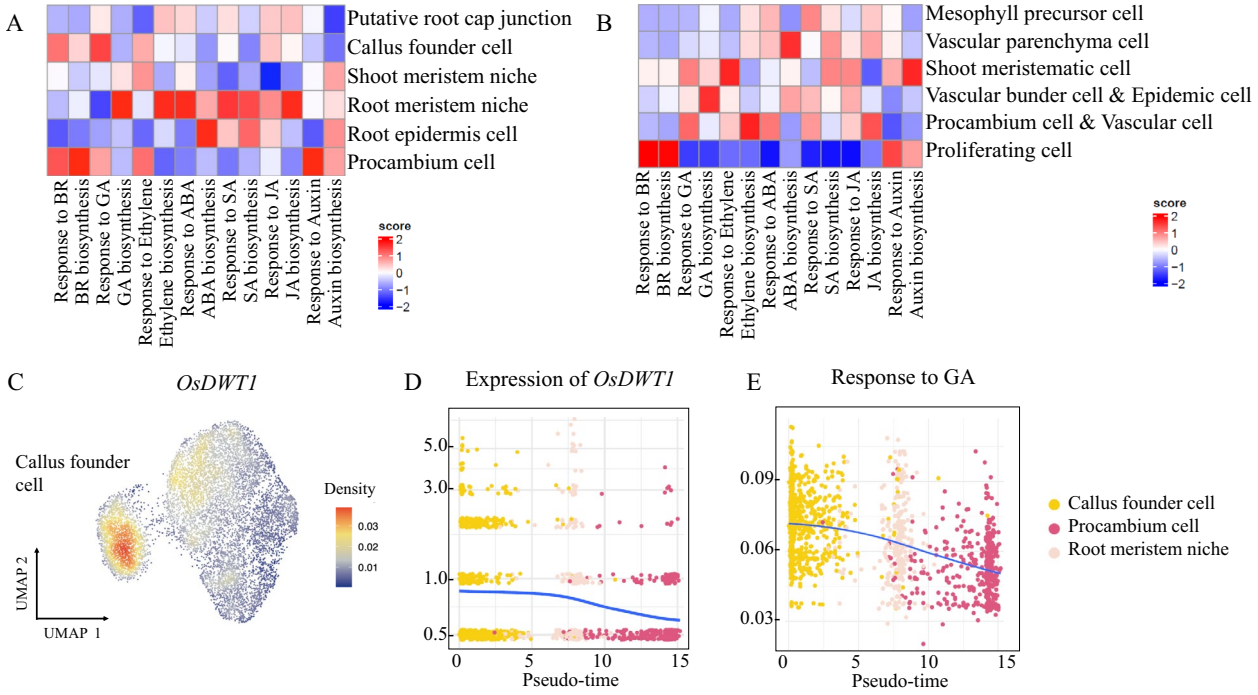


**Fig. 6** The regulatory factors analysis of callus founder cell in rice callus. The expression pattern of genes involved in plant hormones in rice embryonic callus by UCell (**A**). Redder colors indicate higher gene expression levels. The expression pattern of genes involved in plant hormones in rice differentiated callus (**B**). Redder colors indicate higher gene expression levels. The expression pattern of *OsDWT1* in rice embryonic callus (**C**). Redder colors indicate higher gene expression levels. The dynamic expression of *OsDWT1* and the gene sets responding to gibberellin along the pseudo-time of root meristem niche initiation in rice embryonic callus (**D**). Lines represent gene expression levels, and dot denotes cell

pathways in rice [30, 57–60]. As we have found that the callus founder cell represented transcriptionally earliest state of embryonic callus, with *OsDWT1* potentially regulating fate bifurcation—either toward procambium differentiation or developmental arrest—we also note that *dwt1* mutants exhibit reduced expression of the GA synthase gene *ENT-COPALYL DIPHOSPHATE SYNTHASE1* (*OsCPS1*) and elevated expression of the GA deactivator *GIBBERELLIN 2-OXIDASE1* (*OsGA2OS1*), revealing *OsDWT1*'s role in modulating rice stem elongation through GA signaling [60]. This observation raised our suspicion that *OsDWT1* may be associated with the cell fate transition of callus founder cells. We therefore analyzed the expression pattern of *OsDWT1* in embryonic callus, and the result showed that *OsDWT1* was specifically expressed in callus founder cells (Fig. 6C), suggesting a functional role of *OsDWT1* in these initial cellular state cells of embryonic callus. Pseudo-temporal analysis further showed declining *OsDWT1* expression during the transition of callus founder cells into root meristem niche cells (Fig. 6D), which was synchronized with decreased expression of GA-responsive genes (Fig. 6E). Consistently, our bulk RNA-seq data indicate that the gene expression of *OsDWT1* was trended to be suppressed in differentiated callus (Supplemental Table S3). Considering that OsDWT1 is directly or indirectly required for GA signaling to promote cell elongation in rice [50], these results implied that *OsDWT1* is associated with the callus founder cell fate transition.

In conclusion, we constructed a single-cell transcriptome atlas of embryonic callus and differentiated callus, and we identified the callus founder cell as the transcriptionally earliest state that can transit to different cell types in the rice callus. The regulators outlined herein constitute a valuable resource for subsequent investigations.

## Discussion

In this research, we generated a sing-cell transcriptome atlas of embryonic callus and differentiated callus and found that the callus founder cell represents the transcriptionally earliest state of embryonic callus. Furthermore, regulatory factors analysis suggested that *OsDWT1* was associated with the callus founder cell fate transition. Histology is an effective tool for determining the cellular composition and regenerative potential of different callus types derived from rice seed embryos [42, 61]. In this study, we optimized a cryo-section method for potential spatial transcriptomic analysis and characterized embryogenic and differentiated callus at the cellular level to confirm their observed morphological features. Compared with paraffin section, the cryo-section method allows for faster and more convenient preservation of the original morphological characteristics of callus cells. Thus, the cryo-section approach developed in this study

could be applied to analyze the cytological morphology of callus in rice or other species, to illustrate the process of callus differentiation and transformation, and it is not limited to the two culture time points of callus examined in this work.

Studies in the model plant *Arabidopsis* by the Meyerowitz lab have shown that callus resembles the root apical meristem and that ectopic activation of the lateral root developmental program is a common mechanism underlying callus formation from various organs [48]. Research by Zhai et al. categorized *Arabidopsis* callus into three layers—outer, middle, and inner—with the middle layer exhibiting transcriptional features similar to the quiescent center of the root tip and possessing organ regeneration capacity [4]. In this study, cell type annotation of rice callus based on previously reported marker genes revealed that embryonic callus comprised putative root cap junction cells, callus founder cells, shoot meristem niche cells, root meristem niche cells, root epidermis cells, procambium cells. Differentiated callus exhibited mesophyll precursor cells, vascular parenchyma cells, shoot meristematic cells, vascular bunder cells and epidemic cells, procambium and vascular cells, proliferating cells. These differences may be related to the distinct mechanisms of callus formation in *Arabidopsis* (a dicot) and rice (a monocot). Additionally, it should be noted that single-cell transcriptome sequencing enables the identification of low-abundance yet critical marker genes. In this study, trajectory analysis was employed to investigate cell fate transitions, thereby providing supportive evidence for the static classification of callus cell types in a dynamic context. However, this annotation approach for unknown cell types, which relies on known marker genes, still carries inherent potential limitations. Future studies employing techniques such as in situ hybridization, microscopic imaging, flow sorting, and spatial transcriptomics could further resolve callus cell types, providing more substantial validation for the findings of this study.

In rice tissue culture, scutellum-derived callus originates from the epidermal cells of the scutellum, a process that may recruit embryonic developmental mechanisms [15, 43]. In this study, the callus founder cell was induced from rice seed embryos, which continuously divided to form embryonic callus, during which *OsWOX11* was specifically expressed in these cells. It has been reported that *WOX11* is also a callus found cell marker in *Arabidopsis*, which regulates the cell fate transition [23] and is associated with diverse roles in embryogenesis [62]. These observations suggest suggested that the formation of callus founder cell observed in this study also involves the recruitment of embryogenic processes, which is consistent with previous findings [12, 13, 32, 51]. Although our subpopulation analysis of callus founder cells suggests that Subcluster 5 may represent the progenitor subpopulation giving rise to these cells (Fig. 3A-C), we cannot yet definitively determine the cell type identity of Subcluster 5. Whether Subcluster 5 is entirely derived from scutellum-originated cells or represents a novel, previously unknown cell type in rice requires further investigation.

Rice seed germination begins with water imbibition and ends with the emergence of the plumule and radicle. This process requires water, oxygen, a suitable temperature, GA signaling, and the hydrolysis of starch in the endosperm [63]. α-Amylase is a metal hydrolase that requires calcium ions and cleaves α-maltose and α-glucose at random sites along the starch chain [45]. During seed germination, α-amylase is resynthesized in the presence of endogenous GA from the embryo and is positively regulated by GA in the endosperm [25, 45]. *RAmy1A* is expressed in the aleurone layer and endosperm, *RAmy3A* in the endosperm, and *RAmy3E* in the aleurone layer [45, 64]. LTP regulates seed germination by modulating lipid metabolism and transport [51, 65]. *RAmy3D/E* was the marker gene of callus founder cells (Fig. 1E) and studies on the fate transition of these cells into procambium cells indicate that the α-amylase genes *RAmy3A/B/C* may provide energy for the maintenance of callus founder cell cluster by mediating starch hydrolysis, while the lipid transfer protein gene *OsLTP1.15* may regulate lipid transport between transitional cells (Fig. 3D). These findings suggest that the energy source for fate transition in the rice embryonic callus founder cell is analogous to that in the seed germination process.

Studies have shown that the ability of *WOX* genes to broadly regulate growth and developmental processes across different stages and organs in plants is closely associated with the presence of phytohormone-responsive elements in their genomic regions [57, 66]. During rice stem internode development, *OsDWT1* regulates its elongation via the GA pathway [60]. The results of this study indicate that the core regulatory factors of the callus founder cell include key genes such as the GA-induced gene *OsGAE1*, α-amylase genes *RAmy*, and lipid transfer protein gene *LTP*. These genes were enriched during the early development of the callus founder cell into root meristem niche. The expression of *OsDWT1* was synchronized with that of GA-responsive genes during the transition from callus founder cell into root meristem niche (Fig. 6D), suggesting OsDWT1 regulated the callus founder cell transition through GA pathway in rice. Furthermore, the callus founder cell may possess abundant lipid transport activities that regulate the growth of newborn cells and may help regulate cell fate transitions during callus initiation as LRPI-like cells in *Arabidopsis* [3]. In maize, it was reported that GA signal transduction mediated the embryonic callus formation [8]. Considering the expression of OsDWT1 was synchronized with

that of GA-responsive genes during the callus founder cell transited into root meristem niche (Fig. 6D), it is suspected that OsDWT1 regulated the callus founder cell transition through GA pathway in rice.

Lineage tracing is the only way to strictly define an cellular origins. How new cells are produced from initial cellular states has been demonstrated by elegant cell-tracking experiments in the shoot and root meristem [67–69], and recently, lineage tracing via DNA barcoding and multiplexed fluorescence—successful in *Arabidopsis* callus regeneration [70]. However, few reporter lines are available for crops. In our study, we defined the transcriptionally earliest states of embryonic callus and differentiated callus based on the single cell transcriptomic features, which provided prior knowledge of cell-type–specific promoters and genetic manipulation to generate reporter lines in order to verify whether rice callus-derived tissues originate from a single stem cell (the callus founder cell for embryonic callus; the shoot meristematic cell for differentiated callus). Future studies should perturb callus founder cell lineage-specific genes (e.g., *OsWOX11*, *OsDWT1*, *RAmy3A/B/C*, *RAmy3D/E*) to validate single-cell origins and differentiation trajectories. Given that *WOX* genes' broad developmental regulation via phytohormone-responsive elements [57, 66], our finding that *OsDWT1* modulates callus-initiating cell development through GA pathways provides insight for future *WOX* regulatory studies.

## Conclusions

Our results reveal that the callus founder cell represents the transcriptionally earliest state of embryonic callus, which could transit into root meristem niche. This process is associated with starch degradation, lipid transport, energy production and transfer, plant hormones, and flavonoid metabolism, delineated by the single-cell transcriptome atlas of rice embryonic callus. And the analysis of plant hormones and WOX family gene *OsDWT1* across distinct cell populations suggested that GA signaling and *OsDWT1* are associated with the callus founder cell fate transition.

Although not yet fully confirmed by sufficient genetic evidences, the identification of the earliest cell state of rice embryonic callus presented in this study is potentially useful for improving rice genetic transformation and gene editing efficiency of recalcitrant rice varieties through the regulation of cell fate transition.

## Supplementary Information

The online version contains supplementary material available at https://doi.org/10.1186/s12870-026-08596-6.

Supplementary Material 1. Supplemental Fig. S1. The barcode rank plot of rice embryonic callus (A) and differentiated callus (B). Cells are sorted in descending order by UMI count per barcode. The x-axis shows cell barcodes (ranked), and the y-axis displays the corresponding UMI counts. The 'knee' point (blue dashed line) separates high-quality cells from background noise; the red dashed line represents the region of 10,000 cells. (C-D) The scatter plot of the correlation between bulk RNA-seq and pseudo bulk RNA-seq (scRNA-seq) of embryonic callus (C) and differentiated callus (D). The line denotes the trend line.

Supplementary Material 2. Supplemental Fig. S2. The heatmaps of the marker genes of expression pattern across cell clusters in embryonic callus (A) and differentiated callus (B).

Supplementary Material 3. Supplemental Table S1. Key genes of callus founder cell.

Supplementary Material 4. Supplemental Table S2. Genes of rice hormones.

Supplementary Material 5. Supplemental Table S3. Differentially expressed genes identified by bulk RNA-seq.

**Acknowledgements**

We would like to acknowledge Prof. Mengli Xi from the Nanjing Forestry University for providing valuable assistance. We thank the high-performance computing platform of Bioinformatics Center, Nanjing Agricultural University for data analysis.

**Authors' contributions**

Y.W., H.Y. and Z.G. conceived the project. L.L. and Y.W. designed the research. L.L. performed the experiments. W.L., Y.W. and L.L. analyzed the data. L.L. wrote the manuscript. Y.W. and Z.G. revised the manuscript. All authors commented on the article.

**Funding**

This study was supported by the National Key R&D Program of China (2023YFD1200800), Fundamental Research Funds for the Central Universities (KYCXJC2025004), National Natural Science Foundation (31671323) and Jiangsu Collaborative Innovation Center for Modern Crop Production.

**Data availability**

The raw sequence data reported in this paper have been deposited in the Genome Sequence Archive [71] in National Genomics Data Center [72], China National Center for Bioinformation/Beijing Institute of Genomics, Chinese Academy of Sciences (GSA: CRA030608) that are publicly accessible at (https://ngdc.cncb.ac.cn/gsa) . (Reviewer link: https://ngdc.cncb.ac.cn/gsa/s/5F3lDrXa)

## Declarations

**Ethics approval and consent to participate**

Not applicable.

**Consent for publication**

Not applicable.

**Competing interests**

The authors declare no competing interests.

Received: 24 October 2025 / Accepted: 16 March 2026
Published online: 25 March 2026

**References**

1. Adkins SW, Shiraishi T, McComb JA. Rice callus physiology–identification of volatile emissions and their effects on culture growth. Physiol Plant. 1990;78:526.
2. Nishimura S, Maeda E. Histological studies of callus induction in rice seed. Jpn J Crop Sci. 1977;46:275.
3. Yin R, Chen R, Xia K, Xu X. A single-cell transcriptome atlas reveals the trajectory of early cell fate transition during callus induction in Arabidopsis. Plant Commun. 2024;5:100941.
4. Zhai N, Xu L. Pluripotency acquisition in the middle cell layer of callus is required for organ regeneration. Nat Plants. 2021;7:1453.

5. Zhang TQ, Lian H, Zhou CM, Xu L, Jiao Y, Wang JW. A two-step model for de novo activation of WUSCHEL during plant shoot regeneration. Plant Cell. 2017;29:1073.
6. Xu M, Du Q, Tian C, Wang Y, Jiao Y. Stochastic gene expression drives mesophyll protoplast regeneration. Sci Adv. 2021;7:eabg8466.
7. Swapan Kumar T. Optimization of culture variables for efficient callus induction and rapid plant regeneration in zinc rich rice (*Oryza sativa* L.) cv."Chittimuthyalu." J Appl Biol Biotechnol. 2021;9:1.
8. Lowe K, Wu E, Wang N, Hoerster G, Hastings C, Cho MJ, et al. Morphogenic regulators Baby Boom and Wuschel improve monocot transformation. Plant Cell. 2016;28(9):1998.
9. Yang W, Zhai H, Wu F, Deng L, Chao Y, Meng X, et al. Peptide REF1 is a local wound signal promoting plant regeneration. Cell. 2024;187:3024.
10. Jan R, Khan MA, Asaf S, Lee I-J, Kim K-M. Modulation of sugar and nitrogen in callus induction media alter PAL pathway, SA and biomass accumulation in rice callus. Plant Cell Tissue Organ Cult. 2020;143:517.
11. Zhang K, Su J, Xu M, Zhou Z, Zhu X, Ma X, et al. A common wild rice-derived BOC1 allele reduces callus browning in indica rice transformation. Nat Commun. 2020;11:443.
12. Jean-Baptiste K, McFaline-Figueroa JL, Alexandre CM, Dorrity MW, Saunders L, Bubb KL, et al. Dynamics of gene expression in single root cells of *Arabidopsis thaliana*. Plant Cell. 2019;31:993.
13. Wang X, Huang H, Jiang S, Kang J, Li D, Wang K, et al. A single-cell multiomics atlas of rice. Nature. 2025;644:722.
14. Murashige T, Skoog F. A revised medium for rapid growth and bio assays with tobacco tissue cultures. Physiol Plant. 1962;15:473.
15. Guo F, Zhang H, Liu W, Hu X, Han N, Qian Q, et al. Callus initiation from root explants employs different strategies in rice and Arabidopsis. Plant Cell Physiol. 2018;59:1782.
16. Giacomello S, Salmén F, Terebieniec BK, Vickovic S, Navarro JF, Alexeyenko A, et al. Spatially resolved transcriptome profiling in model plant species. Nat Plants. 2017;3:17061.
17. Wolf FA, Hamey FK, Plass M, Solana J, Dahlin JS, Göttgens B, et al. PAGA: graph abstraction reconciles clustering with trajectory inference through a topology preserving map of single cells. Genome Biol. 2019;20:59.
18. La Manno G, Soldatov R, Zeisel A, Braun E, Hochgerner H, Petukhov V, et al. RNA velocity of single cells. Nature. 2018;560:494.
19. Qiu X, Mao Q, Tang Y, Wang L, Chawla R, Pliner HA, et al. Reversed graph embedding resolves complex single-cell trajectories. Nat Methods. 2017;14:97.
20. Andreatta M, Carmona SJ. UCell: robust and scalable single-cell gene signature scoring. Comput Struct Biotechnol J. 2021;19:3796.
21. Liu Q, Liang Z, Feng D, Jiang S, Wang Y, Du Z, et al. Transcriptional landscape of rice roots at the single-cell resolution. Mol Plant. 2021;14:384.
22. Zhang TQ, Chen Y, Liu Y, Lin WH, Wang JW. Single-cell transcriptome atlas and chromatin accessibility landscape reveal differentiation trajectories in the rice root. Nat Commun. 2021;12:2053.
23. Liu J, Sheng L, Xu Y, Li J, Yang Z, Huang H, et al. *WOX11* and 12 are involved in the first-step cell fate transition during de novo root organogenesis in *Arabidopsis*. Plant Cell. 2014;26(3):1081.
24. Toyofuku K, Umemura T, Yamaguchi J. Promoter elements required for sugar-repression of the *RAmy3D* gene for α-amylase in rice. FEBS Lett. 1998;428:275.
25. Song S, Li L, Li Y, Wang T, Fu X. Overexpression of gene OsSUI1 affects floral organ development in rice (*Oryza sativa* L.). Mol Breed. 2017;38(1):4.
26. Suzaki T, Ohneda M, Toriba T, Yoshida A, Hirano HY. *FON2 SPARE1* redundantly regulates floral meristem maintenance with *FLORAL ORGAN NUMBER2* in rice. PLoS Genet. 2009;5:e1000693.
27. Kerstens M, Galinha C, Hofhuis H, Nodine M, Pardal R, Scheres B, et al. PLETHORA transcription factors promote early embryo development through induction of meristematic potential. Development. 2024;151:dev202527.
28. Khan I, Khan S, Zhang Y, Zhou J. Genome-wide analysis and functional characterization of the Dof transcription factor family in rice (*Oryza sativa* L.). Planta. 2021;253:101.
29. Qin H, Wang J, Chen X, Wang F, Peng P, Zhou Y, et al. Rice *OsDOF15* contributes to ethylene-inhibited primary root elongation under salt stress. New Phytol. 2019;223:798.
30. Zhang X, Zong J, Liu J, Yin J, Zhang D. Genome-wide analysis of *WOX* gene family in rice, sorghum, maize, *Arabidopsis* and poplar. J Integr Plant Biol. 2010;52:1016.
31. Lu L, Qiu W, Gao W, Tyerman SD, Shou H, Wang C. *OsPAP10c*, a novel secreted acid phosphatase in rice, plays an important role in the utilization of external organic phosphorus. Plant Cell Environ. 2016;39:2247.
32. Lee S, Chiecko JC, Kim SA, Walker EL, Lee Y, Guerinot ML, et al. Disruption of *OsYSL15* leads to iron inefficiency in rice plants. Plant Physiol. 2009;150:786.
33. Yan M, Fan X, Feng H, Miller AJ, Shen Q, Xu G. Rice OsNAR2.1 interacts with OsNRT2.1, OsNRT2.2 and OsNRT2.3a nitrate transporters to provide uptake over high and low concentration ranges. Plant Cell Environ. 2011;34:1360.
34. Li P, Xue H. Structural characterization and expression pattern analysis of the rice *PLT* gene family. Acta Biochim Biophys Sin. 2011;43:688.
35. Zhang TQ, Chen Y, Wang JW. A single-cell analysis of the *Arabidopsis* vegetative shoot apex. Dev Cell. 2021;56:1056.
36. Wang Y, Huan Q, Li K, Qian W. Single-cell transcriptome atlas of the leaf and root of rice seedlings. J Genet Genomics. 2021;48:881.
37. Ito Y, Kimura F, Hirakata K, Tsuda K, Takasugi T, Eiguchi M, et al. Fatty acid elongase is required for shoot development in rice. Plant J. 2011;66:680.
38. Ishibashi T, Kimura S, Sakaguchi K. A higher plant has three different types of RPA heterotrimeric complex. J Biochem. 2006;139:99.
39. Scarpella E, Rueb S, Boot KJM, Hoge JHC, Meijer AH. A role for the rice homeobox gene *Oshox1* in provascular cell fate commitment. Development. 2000;127:3655.
40. Ito Y, Kurata N. Disruption of *KNOX* gene suppression in leaf by introducing its cDNA in rice. Plant Sci. 2008;174:357.
41. Fang J, Yuan S, Li C, Jiang D, Zhao L, Peng L, et al. Reduction of ATPase activity in the rice kinesin protein Stemless Dwarf 1 inhibits cell division and organ development. Plant J. 2018;96:620.
42. Bevitori R, Popielarska-Konieczna M, Dos Santos EM, Grossi-de-Sá MF, Petrofeza S. Morpho-anatomical characterization of mature embryo-derived callus of rice (*Oryza sativa* L.) suitable for transformation. Protoplasma. 2014;251:545.
43. Guo F, Wang H, Lian G, Cai G, Liu W, Zhang H, et al. Initiation of scutellum-derived callus is regulated by an embryo-like developmental pathway in rice. Commun Biol. 2023;6:457.
44. Guiderdoni E, Cordero MJ, Vignols F, Garcia-Garrido JM, Lescot M, Tharreau D, et al. Inducibility by pathogen attack and developmental regulation of the rice *Ltp1* gene. Plant Mol Biol. 2002;49:679.
45. Damaris RN, Lin Z, Yang P, He D. The rice alpha-amylase, conserved regulator of seed maturation and germination. Int J Mol Sci. 2019;20:450.
46. Kamarudin ZS, Yusop MR, Ismail MR, Tengku Muda Mohamed M, Harun AR, Yusuff O, et al. LEA gene expression assessment in advanced mutant rice genotypes under drought stress. Int J Genomics. 2019;2019:8406036.
47. Ikeuchi M, Sugimoto K, Iwase A. Plant callus: mechanisms of induction and repression. Plant Cell. 2013;25:3159.
48. Sugimoto K, Jiao Y, Meyerowitz EM. *Arabidopsis* regeneration from multiple tissues occurs via a root development pathway. Dev Cell. 2010;18:463.
49. Jain M, Tyagi AK, Khurana JP. Genome-wide analysis, evolutionary expansion, and expression of early auxin-responsive SAUR gene family in rice (*Oryza sativa*). Genomics. 2006;88:360.
50. Jan A, Kitano H, Matsumoto H, Komatsu S. The rice OsGAE1 is a novel gibberellin-regulated gene and involved in rice growth. Plant Mol Biol. 2006;62:439.
51. Vignols F, Wigger M, Garćıa-Garrido JM, Grellet F, Kader J-C, Delseny M. Rice lipid transfer protein (LTP) genes belong to a complex multigene family and are differentially regulated. Gene. 1997;195:177.
52. Sylvester AW, Smith L, Freeling M. Acquisition of identity in the developing leaf. Annu Rev Cell Dev Biol. 1996;12:257.
53. Li W, Wu J, Weng S, Zhang Y, Zhang D, Shi C. Identification and characterization of dwarf 62, a loss-of-function mutation in DLT/OsGRAS-32 affecting gibberellin metabolism in rice. Planta. 2010;232:1383.
54. Yamanouchi U, Yano M, Lin H, Ashikari M, Yamada K. A rice spotted leaf gene, Spl7, encodes a heat stress transcription factor protein. Proc Natl Acad Sci U S A. 2002;99:7530.
55. Selby R, Jones DS. Complex peptide hormone signaling in plant stem cells. Curr Opin Plant Biol. 2023;75:102442.
56. Jiang K, Guo H, Zhai J. Interplay of phytohormones and epigenetic regulation: a recipe for plant development and plasticity. J Integr Plant Biol. 2022;65:381.
57. Somssich M, Je BI, Simon R, Jackson D. CLAVATA-WUSCHEL signaling in the shoot meristem. Development. 2016;143:3238.
58. Wu X, Dabi T, Weigel D. Requirement of homeobox gene STIMPY/WOX9 for Arabidopsis meristem growth and maintenance. Curr Biol. 2005;15:436.
59. Zhang N, Bitterli P, Oluoch P, Hermann M, Aichinger E, Groot EP, et al. Deciphering the molecular logic of WOX5 function in the root stem cell organizer. EMBO J. 2024;44:281.
60. Wang W, Li G, Zhao J, Chu H, Lin W, Zhang D, et al. DWARF TILLER1, a w uschel-related homeobox transcription factor, is required for tiller growth in rice. PLoS Genet. 2014;10:e1004154.

61. Vega R, Vásquez N, Espinoza A, Gatica-Arias A, Valdez M. Histology of somatic embryogenesis in rice (*Oryza sativa* cv. 5272). Rev Biol Trop. 2009;57:141.
62. Wan Q, Zhai N, Xie D, Liu W, Xu L. Wox11: the founder of plant organ regeneration. Cell Regen. 2023;12:1.
63. Hong YF, Ho TH, Wu CF, Ho SL, Yeh RH, Lu CA, et al. Convergent starvation signals and hormone crosstalk in regulating nutrient mobilization upon germination in cereals. Plant Cell. 2012;24:2857.
64. Huang N, Chandler J, Thomas BR, Koizumi N, Rodriguez RL. Metabolic regulation of α-amylase gene expression in transgenic cell cultures of rice (*Oryza sativa* L.). Plant Mol Biol. 1993;23:737.
65. Kim TH, Kim MC, Park JH, Han SS, Kim BR, Moon BY, et al. Differential expression of rice lipid transfer protein gene (LTP) classes in response to abscisic acid, salt, salicylic acid, and the fungal pathogen *Magnaporthe grisea*. J Plant Biol. 2006;49:371.
66. Cheng S, Tan F, Lu Y, Liu X, Li T, Yuan W, et al. WOX11 recruits a histone H3K27me3 demethylase to promote gene expression during shoot development in rice. Nucleic Acids Res. 2018;46:2356.
67. Stewart RN, Dermen H. Determination of number and mitotic activity of shoot apical initial cells by analysis of mericlinal chimeras. Am J Bot. 1970;57:816.
68. Birnbaum K, Shasha DE, Wang JY, Jung JW, Lambert GM, Galbraith DW, et al. A gene expression map of the Arabidopsis root. Science. 2003;302:1956.
69. Birnbaum K, Jung JW, Wang JY, Lambert GM, Hirst JA, Galbraith DW, et al. Cell type–specific expression profiling in plants via cell sorting of protoplasts from fluorescent reporter lines. Nat Methods. 2005;2:615.
70. Lu X, Zhang Q, Wang Z, Cheng X, Yan H, Cai S, et al. Development of an inducible DNA barcoding system to understand lineage changes in Arabidopsis regeneration. Dev Cell. 2025;60:305.
71. Chen T, Chen X, Zhang S, Zhu J, Tang B, Wang A, et al. The genome sequence archive family: toward explosive data growth and diverse data types. Genomics Proteomics Bioinformatics. 2021;19:578.
72. CNCB-NGDC Members and Partners. Database resources of the national genomics data center, China National Center for Bioinformation in 2025. Nucleic Acids Res. 2025;53:D30.

## Publisher's Note